Organic & Biomolecular Chemistry

Accepted Manuscript

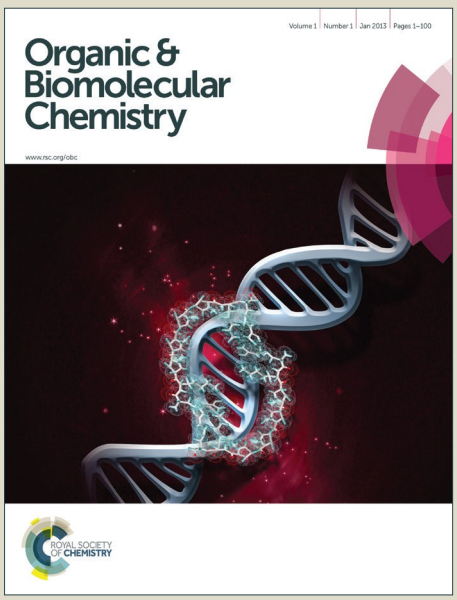

ROYAL SOCIETY OF CHEMISTRY

www.rsc.org/obc

Journal Name

ARTICLE

Quinolone-1-(2*H*)-ones as Hedgehog Signalling Pathway Inhibitors

Trieu N. Trinh,[a] Eileen A. McLaughlin,[b,†] Mohammed Abdel-Hamid,[a,c] Christopher P. Gordon,[d] Ilana R. Bernstein,[b] Victoria Pye,[b] Peter Cossar,[a] Jennette A. Sakoff,[e] and Adam McCluskey[a*]

Received 00th January 20xx,

Accepted 00th January 20xx

DOI: 10.1039/x0xx00000x

www.rsc.org/

A series of quinolone-2-(1*H*)-ones derived from a Ugi-Knoevenagel three- and four- component reaction were prepared exhibiting low micromolar cytotoxicity against a panel of eight human cancer cell lines known to possess the Hedgehog Signalling Pathway (HSP) components, as well as the seminoma TCAM-2 cell line. A focused SAR study was conducted and revealed core characteristics of the quinolone-2-(1*H*)-ones required for cytotoxicity. These requirements included a C3-tethered indole moiety, an indole C5-methyl moiety, an aliphatic tail or an ester, as well as an additional aromatic moiety. Further investigation in the SAG-activated Shh-LIGHT 2 cell line with the most active analogues: 2-(3-cyano-2-oxo-4-phenylquinolin-1(2*H*)-yl)-2-(1-methyl-1*H*-indol-3-yl)-*N*-(pentan-2-yl)acetamide (**5**), 2-(3-cyano-2-oxo-4-phenylquinolin-1(2*H*)-yl)-2-(5-methyl-1*H*-indol-3-yl)-*N*-(pentan-2-yl)acetamide (**23**) and ethyl (2-(3-cyano-2-oxo-4-phenylquinolin-1(2*H*)-yl)-2-(5-methyl-1*H*-indol-3-yl)acetyl)glycinate (**24**) demonstrated a down regulation of the HSP via a reduction in Gli expression, and in the mRNA levels of $Ptch_1$ and Gli_2. Analogues **5**, **23** and **24** returned in cell inhibition values of 11.6, 2.9 and 3.1 μM, respectively, making this new HSP-inhibitor pharmacophore amongst the most potent non-Smo targeted inhibitors thus far reported.

Introduction

The Hedgehog (Hh) signalling pathway (HSP) plays a pivotal role in embryogenesis by controlling the spatial and temporal regulation of cell proliferation, differentiation, and tissue patterning.[1, 2] Aberrant Hh signalling in humans can initiate the development of a diverse range of human cancers, including basal cell carcinoma,[3] medulloblastoma,[4-6] cancers of the pancreas,[7] prostate,[8] lung,[9, 10] colon,[11] stomach,[12] breast,[13, 14] ovary [15] and perhaps most problematically the formation of cancer stem cells.[16, 17] Consequently, suppressing the HSP is an attractive and recently validated chemotherapeutic target with two inhibitors targeting the Smoothened (Smo) protein, Vismodegib (**1**, GDC-0449, Erivedge®) and Sonidegib (**2**, LDE225, Odomzo®) (Figure 1), approved by FDA for the treatment of early and advanced basal cell carcinomas.[18, 19]

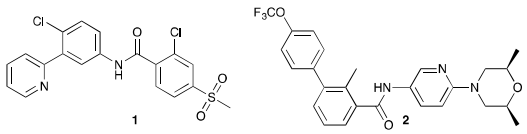

Figure 1. Chemical structures of the Smo inhibitors Vismodegib (**1**, GDC-0449, Erivedge®) and Sonidegib (**2**, LDE225, Odomzo®) approved by FDA for the treatment of early and advanced basal cell carcinomas.[18, 19]

The activation and suppression of the HSP involves an intricate interplay between proteins, both within the HSP and with associated signalling networks including the TGF-β, p53, WIP1, PI3K/AKT and RAS/MEK pathways. Briefly, the canonical HSP functions in a hierarchical manner, in which a Hedgehog ligand (Sonic, Desert or Indian hedgehog protein) binds to the membrane receptor $Patched_1$ ($Ptch_1$), resulting in the activation of the Smo protein and subsequent release of active Glioma-Associated Oncogene Homolog transcriptional factors (Gli_{1-3}) into the nucleus.[1, 2, 20] These Gli transcription factors facilitate the transcription of Hh target genes, including the components of the HSP Gli_1, Gli_2, $Ptch_1$, and $Ptch_2$.[21] Alternatively, the HSP can be activated directly at the Smo level via a synthetic Smo agonist (**3**, SAG) (Figure 2).[22]

[a] *Chemistry, Priority Research Centre for Chemical Biology, University of Newcastle, University Drive Callaghan NSW 2308, Australia. * Phone: +61(2)49 216486; Fax: +61(2)49 215472; Email: Adam.McCluskey@newcastle.edu.au*
[b] *Biology, Priority Research Centre for Chemical Biology, University of Newcastle, University Drive Callaghan NSW 2308, Australia.*
[c] *Department of Medicinal Chemistry, Faculty of Pharmacy, Assiut University, Assiut 71526, Egypt*
[d] *Nanoscale Organization and Dynamics Group, School of Science and Health, University of Western Sydney, Penrith South DC, NSW, Australia.*
[e] *Department of Medical Oncology, Calvary Mater Hospital, Edith Street, Waratah, NSW 2298, Australia*
[f] *† Current Address: School of Biological Sciences, University of Auckland, Auckland, New Zealand.*

Electronic Supplementary Information (ESI) available: NMR, IR, mass spectra, and HPLC peaks. See DOI: 10.1039/x0xx00000x

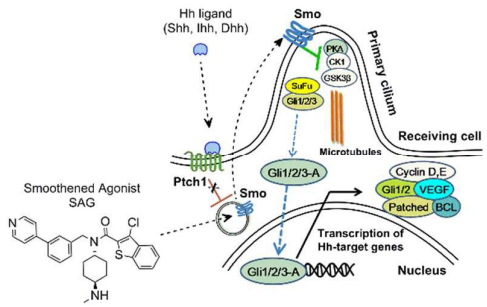

Figure 2. The canonical HSP is initiated by the binding of the Hedgehog ligand (Sonic, Desert or Indian) to the membrane receptor $Ptch_1$, resulting in the activation of Smo protein and release of active Gli transcriptional factors (Gli_{1-3}) into the nucleus, culminating in the transcription of Hh-target genes.[20] Alternatively, the HSP can be activated directly at the Smo level by using SAG (**3**).[22]

The hierarchical character of the HSP, affords several opportunities to suppress the pathway including the inhibition of Hedgehog-ligand-$Ptch_1$ interactions,[23, 24] inhibition of the Smo protein [22, 25-35] or further downstream such as the inhibition of the Gli transcription factors.[36-46] At present the most clinically advanced HSP inhibitor compounds target Smo. These clinical studies have identified limitations to this approach including the development of acquired resistance resulting from Smo mutations and compensatory amplification of Gli_2 transcription factors by the aforementioned interacting pathways.[20] Targeting the HSP further downstream of Smo at the Gli transcription factor level, and/or indirectly at interacting signalling pathways may constitute a more robust strategy for treating HSP related cancers.[20, 43]

Given our ongoing interest in the development of small molecule HSP inhibitors [20, 47] our attention was drawn to the previously reported HIP-4 (**4**).[43] Considered as a non-selective inhibitor of the Gli family of transcription factors, HIP-4 contained a number of structural features present within a family of quinolone-2-(1*H*)-ones recently reported from our laboratories (exemplified by **5**; Figure 3).[48]

To assess the potential of quinolone-1-(*2H*)-one scaffold as HSP inhibitors, we first evaluated their cytotoxicity in a double-filter screening against a panel of eight human cancer cell lines possessing components of the HSP (Table 1; entries 1-8), and one seminoma cancer cell line (TCAM-2) (Table 1; entry 9).

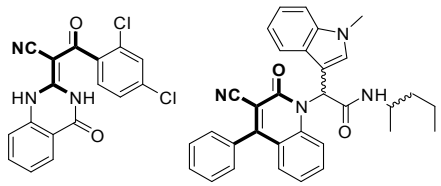

4
HPI-4

5

Figure 3. N-(sec-butyl)-2-(3-cyano-2-oxo-4-phenylquinolin-1-(2*H*)-yl)-2-(1-methyl-1*H*-indol-3-yl)acetamide (**5**) from our laboratory with the bolded structure sections reflecting the structural similarities with the Gli inhibitor HPI-4 (**4**).

The TCAM-2 cell line, in addition to expressing the HSP (ESI†), possesses the active PI3K signalling pathway [49] and the aberrantly up-regulated mitogen-activated protein kinase signalling pathway (RAS/RAF/MEK/ERK) due to a mutation at the BRAF gene (V600E).[50-52] Together these signalling pathways create a complex loop facilitating the non-canonical activation of Gli activity downstream of Smo.[47, 49, 53] Thus the TCAM-2 cell line provides a valuable filter to identify potential Gli transcription factor inhibitors, with this (we believe) to be the first such use of this system. Active compounds from our double-filter cytotoxicity screening approach would be further evaluated in SAG-activated Sonic Hedgehog-(Shh) LIGHT 2 cell line model for their potential to suppress the HSP using Dual Luciferase Reporter (DLR), Reverse Transcription PCR (RT-PCR) and Quantitative PCR (qPCR) assays.

Table 1. Human cancer cell lines known to possess the HSP.

Entry	Cell Line	Cell Type	HSP components expressed	Ref
1	HT29	Colorectal carcinoma	Ihh, Shh, $Ptch_1$, Smo, $Gli_{1,2,3}$, Hhip at mRNA levels	54
2	SW480	Colorectal carcinoma	Shh, Ptch, Smo, Sufu, $Gli_{2,3}$, Hhip at mRNA levels	55
3	MCF-7	Breast adenocarcinoma	Ihh, Shh, Dhh, Ptch1, Smo, $Gli_{1,2}$ at mRNA levels	14
4	A2780	Ovarian carcinoma	Shh, Dhh, Ptch, Smo, Gli_1 at mRNA and protein levels	15
5	H460	Lung carcinoma	Smo, $Ptch_1$, Gli_1 at mRNA levels	56, 57
6	DU145	Prostate carcinoma	$Ptch_1$, $Gli_{1,2}$ at mRNA levels	58, 59
7	BE2-C	Neuroblastoma	Shh, Smo, Gli_2 at protein levels	60
8	MIA-Paca-2	Pancreatic carcinoma	Shh, $Ptch_{1,2}$, Smo, $Gli_{1,2}$ at mRNA levels	61,62
9	TCAM-2	Seminoma	Ptch1, Smo, SuFu, Gli2, and Gli3 at mRNA levels	ESI†
			Expression of PI3 pathway	49
			Mutation at BRAF gene, overexpression of RAS/RAF/MEK/ERK pathway	51,50, 52

Results and discussion

A targeted library of quinolone-1-(2*H*)-ones retaining the highlighted pharmacophore of **4** (Figure 3) was prepared using our previously reported sequential Ugi-Knoevenagel protocol.[48] In a typical synthesis, a methanolic solution of 2-aminobenzophenone (**6**), 4-chlorobenzaldehyde (**7**), cyanoacetic acid (**8**) and ethyl isocyanate (**9**) in methanol was stirred at room temperature for 48 h, followed by chromatographic separation of the desired product (**10**) (Scheme 1).[48] Using this approach eleven exemplars were generated, of which five (**5**, **12**, **14**-**16**, Table 2) were obtained as a mixture of diastereomers (see experimental).

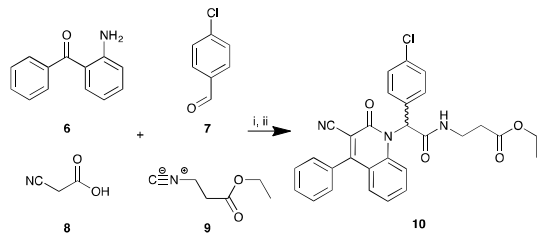

Scheme 1. Synthesis of quinolone-2-(1*H*)-ones. Reagents and Conditions: (i) MeOH, rt; (ii) spontaneous.[48]

Attempts to separate individual diastereomers proved unsuccessful. However using Willoughby et al's computational approach we identified the relative configuration of the major isomers in each instance.[63] With analogues **14**-**16** the geometry was optimised and free energy calculated using Density Functional Theory and B3LYP (6-31+G(d,p) basis set) approaches. This theory level was used to calculate the ^{1}H NMR shifts of each conformer and to predict the more abundant diasteroisomer obtained synthetically. Data relating to analogues **14**-**16** showed distinguishable ^{1}H NMR peaks for each pair of diastereomersfor the two methyl and the methylene moieties of the 2-pentyl substituent. Comparison of the R,S/S,R and R,S/S,R pairs as well as their computed ^{1}H NMR chemical shifts (ESI, Table S1) showed favourable DFT energies for the R,S/S,R pair compared to R,R/S,S (difference of 1.6 - 4.3 kcal/mol) in all instances. This was consistent with the observed ^{1}HNMR shifts for the major product and the calculated chemical shifts for R,S/S,R pair of enantiomers. This 11 component library was screened against our panel of eight human cancer cell lines and the data presented in Table 2.

Table 2. Evaluation of the cytotoxicity of the quinolin-2-(1*H*)-ones analogues (**5, 10-19**) against a panel of eight hedgehog signalling pathway expressing cancer cell lines. Values are the percentage of growth inhibition at 25 μM drug concentration

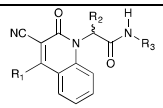

Compound	R_1	R_2	R_3	HT29[a]	SW480[a]	MCF-7[b]	A2780[c]	H460[d]	Du145[e]	BE2-C[f]	MIA[g]
5				79 ± 2	99 ± 5	92 ± 2	96 ± 2	84 ± 4	94 ± 4	92 ± 2	92 ± 2
10			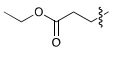	49 ± 2	43 ± 3	62 ± 3	51 ± 2	43 ± 7	22 ± 2	42 ± 0	41 ± 2
11				42 ± 3	57 ± 1	60 ± 5	38 ± 5	32 ± 4	28 ± 4	43 ± 6	45 ± 10
12				34 ± 6	46 ± 1	65 ± 2	39 ± 6	26 ± 7	18 ± 2	41 ± 2	39 ± 15
13				11 ± 7	2 ± 5	20 ± 5	27 ± 3	4 ± 4	<0	8 ± 3	16 ± 10
14				11 ± 6	7 ± 2	11 ± 4	29 ± 3	5 ± 5	<0	<0	14 ± 11
15				46 ± 1	47 ± 5	29 ± 3	31 ± 1	28 ± 7	<0	42 ± 3	36 ± 2
16				85 ± 0	77 ± 3	90 ± 2	96 ± 1	>100	63 ± 4	>100	81 ± 0
17				18 ± 3	3 ± 9	17 ± 3	35 ± 1	14 ± 12	<0	<0	19 ± 3
18				38 ± 3	26 ± 7	45 ± 5	42 ± 3	26 ± 17	21 ± 5	16 ± 1	30 ± 3
19				6 ± 2	6 ± 3	9 ± 9	19 ± 6	9 ± 5	4 ± 5	2 ± 7	14 ± 5

[a] HT29 and SW480 (colon carcinoma); [b] MCF-7 (breast carcinoma); [c] A2780 (ovarian carcinoma); [d] H460 (lung carcinoma); [e] Du145 (prostate carcinoma); [f] BE2-C (neuroblastoma); [g] MIA (pancreatic carcinoma).

Analysis of the data presented in Table 2 showed analogues **5** and **16** as the most promising at the 25 μM drug concentration evaluated. The C3-tethered indole group (**5**) was shown to be crucial for activity, while its replacement by either a 4-methoxyphenyl (**12**) or phenyl moiety (**14**) resulted in a significant decrease in inhibition. All other analogues displayed modest (30-75%) to negligible growth inhibition (<30%) (Table 2). The two most promising analogues (**5** and **16**) proceeded to full dose response evaluation (Table 3).

Journal Name

ARTICLE

Table 3. Evaluation of the cytotoxicity, GI_{50} values (μM), of compounds **5** and **16** against a panel of nine human HSP expressing cancer cell lines. GI_{50} is the concentration of drug that reduces cell growth by 50%.

Compound	HT29[a]	SW480[a]	MCF-7[b]	A2780[c]	H460[d]	Du145[e]	BE2-C[f]	MIA[g]	TCAM-2[h]
5	5.3 ± 0.3	11 ± 1	4.6 ± 1.1	3.9 ± 0.3	5.2 ± 0.1	13 ± 0	3.6 ± 0.1	6.0 ± 0.1	11.6 ± 0.6
16	8.7 ± 0.5	17 ± 1	7.9 ± 1	7.5 ± 0.6	11 ± 1	18 ± 1	7.3 ± 0.3	13 ± 1	>100

[a] HT29 and SW480 (colon carcinoma); [b] MCF-7 (breast carcinoma); [c] A2780 (ovarian carcinoma); [d] H460 (lung carcinoma); [e] Du145 (prostate carcinoma); [f] BE2-C (neuroblastoma); [g] MIA (pancreatic carcinoma).

The data in Table 3 shows **5** and **16** to be potent broad spectrum cytotoxic agents with GI_{50} values of 3.6-11 and 7.3-18 μM for respectively. However examination of these two analogues in TCAM-2 cells revealed **16** to be inactive (GI_{50} >100 μM), while the indole-based **5** displayed excellent growth inhibition (GI_{50} = 11.6 ± 0.6 μM). These data and those presented in Table 2 support retention of the indole moiety as a key pharmacophore in this study. To further investigate this hypothesis we developed a second indole moiety based focused library, assembled via our Ugi-Knoevenagel approach (Scheme 1). Given the differential activity noted with the TCAM-2 cell line, these new indole based analogues were screened directly in this cell line only and the data presented in Table 4. This represents the first such use of TCAM-2 cells in the development of HSP inhibitors.

Table 4. Synthesis results and the evaluation of the cytotoxicity of the second focused library against the TCAM-2 cell line. Values are the percentage of growth inhibition at 10 μM drug concentration and GI_{50} were determined where the growth inhibition > 50% (ESI†) ***Reagents and conditions:*** (***i***) MeOH, rt, 24 h

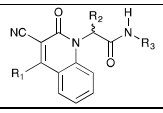

Compound	R_1	R_2	R_3	Yield (%)	TCAM-2 % Inhibition at 10 µM	TCAM-2 GI_{50} (µM)
5				38	52	11.6 ± 0.6
20				13	21	-
21				11	41	-
22				36	<0	-
23				46	72	2.9 ± 0
24				34	66	3.1 ± 0.4
25		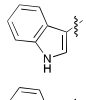		46	28	-
26				26	45	-
27			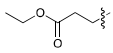	50	44	-
28				33	<0	-
29				47	41	-
30				26	44	

Analysis of the DLR assay data indicated moderate suppression (55, 54 and 31%) of Gli expression at the protein level by **5**, **23** and **24** respectively relative to the DMSO and SAG-treated controls (Figure 4). This inhibition over Gli protein expression does not always result from the suppression of the HSP due to the complex crosstalk of interacting signalling pathways sharing Gli_2 as the same effector.[20]

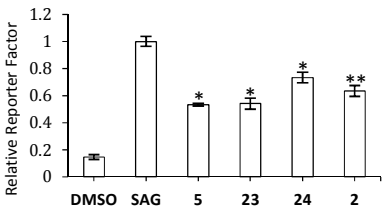

Figure 4: Effect of compounds **5**, **23**, and **24** at 25 µM and Sonidegib (**2**) at 100nM concentration on the suppression Gli expression in Shh-LIGHT2 cells activated with 100nM SAG. Treatments were performed in triplicate. *P < .05, ** P < .001 compared with SAG control

Thus, the mRNA level of HSP components in SAG-activated Shh-LIGHT2 cell line was probed using a combination of Reverse Transcription PCR (RT-PCR) and Quantitative PCR (qPCR) assays. Of the individual HSP components identified at the mRNA level by RT-PCR, only *$Ptch_1$* and *Gli_2* exhibited significant up-regulation under SAG-stimulation (ESI†) and thus became our targets. Unlike previous reports, we found no evidence for Gli_1 expression under the conditions evaluated herein.[65, 66] The outcomes of our qPCR analysis of $Ptch_1$ and Gli_2 post treatment at 10 µM of **5**, **23** and **24** are shown in Figure 5.

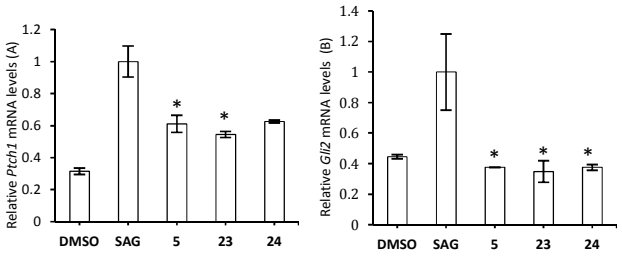

Figure 5. Effect of compounds **5**, **23**, and **24** at 10 μM concentration on mRNA levels of *Ptch*$_1$ (**A**) and *Gli*$_2$ (**B**) in Shh-LIGHT2 cells activated with 100nM SAG. Treatments were performed in triplicate. * $P < .05$ compared to SAG controls.

As illustrated in Figure 5 both *Ptch*$_1$ and *Gli*$_2$ mRNA levels were significantly suppressed by compounds **5**, **23**, and **24** at 10μM treatments. To clarify the data presented in Figure 5 the percent inhibition of *Ptch*$_1$ and *Gli*$_2$ mRNA levels were calculated (Table 5), in which the inhibition of mRNA levels of *Gli*$_2$ appeared to be larger than 100%. This may arise as a result of the compounds not only suppressing the elevated mRNA levels of *Gli*$_2$ induced by SAG, but also inhibition of *Gli*$_2$ in inactivated Shh LIGHT2 cells. Together, these results indicate that compounds **5**, **23**, and **24** exhibited suppressive activity over the HSP in Shh LIGHT2 through the inhibition of *Ptch*$_1$ at mRNA level and Gli$_2$ at both mRNA and protein levels.

Table 5. Evaluation of compounds **5, 23,** and **24** (10 μM) on Ptch$_1$ and Gli$_2$ mRNA levels in SAG-activated Shh-LIGHT 2 cells. Values are the approximate percentage reduction relative to the DMSO and SAG-treated controls.

Compound	Percent change in Ptch$_1$ and Gli$_2$ mRNA levels (%)	
	Ptch$_1$	**Gli$_2$**
5	57	112
23	67	117
24	55	112

Conclusions

We have successfully identified a new scaffold of HSP inhibitors derived from the Ugi-Knoevenagel products. At inhibitor concentration of 10 μM, these quinolone-2-(1*H*)-one analogues can effectively inhibit the mRNA levels of Ptch$_1$ and Gli$_2$ in Sonic Hedgehog LIGHT2 cell line stimulated with 100nM SAG. Of note, selected compounds demonstrated good cytotoxicity (GI_{50} from 2.9 to 18.0 μM) against a panel of eight human cancer cell lines, as well as the mutant seminoma TCAM-2 cell line, all of which are known to possess the HSP's components (Table 3). Whilst the exact mechanism remains to be determined, our data is consistent with inhibition downstream of Smo due to the fact that it is valid in the presence of SAG, a potent Smo activator. Moreover, the analogues reported herein suppress *Gli2* mRNA level in non-activated Shh LIGHT 2 cells also supports a downstream of Smo inhibition. Inhibition of Smo does not display this phenotype. Furthermore, a preliminary quinolone-2-(1*H*)-one pharmacophore required to elicit the cytotoxicity profile has been established. Apparent crucial structural features include an indole moiety at R_2 which is tethered to the remainder of the scaffold through the C3 position. Moreover, the presence of bulky aliphatic groups within R_3 of the scaffold appears to be required to endow cytotoxicity against the TCAM-2 cell line. These valuable data undoubtedly will enable us to exploit the current pharmacophore to develop next generation analogues with superior properties to combat the hedgehog signalling related cancers. The results of these efforts will be reported in due course.

Experimental section

Biology

Cell culture and stock solutions

Stock solutions were prepared as follows and stored at -20ºC: Related compounds were stored as 40 mM solutions in DMSO. All cell lines were cultured at 37ºC in an automated CO_2 (5%) incubator (HERA cell 150, Thermo Scientific).

HT29, SW480 (colon carcinomas), MCF-7 (breast carcinoma), A2780 (ovarian carcinoma), H460 (lung carcinoma), A431 (skin carcinoma), DU145 (prostate carcinoma), BEC-2 (neuroblastoma), SJ-G2 (glioblastoma) and MIA (pancreatic carcinoma) cell lines were maintained in Dulbecco's modified Eagle's medium (Trace Biosciences, Australia) supplemented with 10% foetal bovine serum, 10 mM sodium bicarbonate, penicillin (100 IU/mL), streptomycin (100 mg/mL), and glutamine (4 mM).

TCAM-2 cell line (testis carcinoma) was maintained in Hyclone RPMI 1640 medium (GE Healthcare Life Sciences) supplemented with 10% foetal bovine serum (Gibco®), penicillin (100 IU/mL) (Gibco®), streptomycin (100 mg/mL) (Gibco®) and glutamine (4 mM) (Gibco®).

Shh LIGHT2 cell line (derived from NIH-3T3 fibroblast cell line) was maintained in Gibco® Dulbecco's modified Eagle's medium (Thermo Fisher Scientific) supplemented with 10% foetal bovine serum (FBS), glutamine (4mM), Zeocin® (0.15mg/mL, Invitrogen), Genetecin® (0.4mg/mL, Thermo Fisher Scientific).

In vitro growth inhibition assay

Protocol 1 (HT29, SW480, MCF-7, A2780, H460, DU145, BEC-2 and MIA cell lines)

Cells in logarithmic growth were transferred to 96-well plates. Cytotoxicity was determined by plating cells in duplicate in 100 μL medium at a density of 2500-4000 cells/well. On day 0, (24 h after plating) when the cells were in logarithmic growth, 100 μL medium with or without the test agent was added to each well. After 72 h drug exposure growth inhibitory effects were evaluated using the MTT (3-[4,5-dimethylthiazol-2-yl]-2,5-diphenyl-tetrazolium bromide) assay and absorbance read at 540 nm. Percentage growth inhibition was determined at a fixed drug concentration of 25 μM. A value of 100% is indicative of total cell growth inhibition. Those analogues showing appreciable percentage growth inhibition underwent further dose response analysis allowing for the calculation of a GI_{50} value. This value is the

drug concentration at which cell growth is 50% inhibited based on the difference between the optical density values on day 0 and those at the end of drug exposure.

Protocol 2 (TCAM-2 cell line)

Cells in logarithmic growth were transferred to 96-well plates in triplicates at 2500 cells/well in 200µL media and cultured in the automated CO_2 (5%) incubator. When the cells reach to about 80% confluency, old media were removed and replaced with 100 µL fresh media containing testing agents (at 10 µM), as well as DMSO and 1% Triton X as controls. Cells were further incubated for another 72 h and were evaluated using the MTT assay with the absorbance at 550 nm. The growth inhibition was calculated based on the differences in the optical densities between those treated by various agents (10 µM) *and* controls by DMSO and 1% Triton X treatments. Only those agents which expressed a growth inhibition greater than 60% were further subjected to full dose response evaluation (GI_{50} values).

Dual Luciferase Reporter assay

Shh-LIGHT2 cells in logarithmic growth were transferred to 96-well plate (3000 cells/well) and cultured to confluency. The Shh-LIGHT2 cells were then grown in DMEM containing 0.5% FBS, 4 mM glutamine, 0.15 mg/mL Zeocin®, 0.4 mg/mL Genetecin®, and combinations of 100 nM SAG (Smo agonist), with different testing compounds (**5, 23**, and **24**) at 25 µM each. The SAG- free DMSO treated (25 µM), and SAG-included Sonidegib (100nM) treated cells were used as controls. Treatments were done in triplicates. After the cells were cultured for another 45 h in the automated CO_2 (5%) incubator, the resulting firefly and Renilla luciferase activities were measured using a Dual Luciferase Reporter kit (Promega) and a BMG Labtech Pherastar microplate reader (Thermo Fisher Scientific).

RNA Extraction

Total RNA was isolated from cultured cells using two rounds of a modified acid guanidinium thiocyanate-phenol-chloroform protocol:[67] washed cells resuspended in lysis buffer (4 M guanidinium thiocyanate, 25 mM sodium citrate, 0.5% sarkosyl, 0.72% β-mercaptoethanol). RNA was isolated by phenol/chloroform extraction and isopropanol precipitated.

Reverse Transcription PCR (RT-PCR) and Quantitative PCR (qPCR)

Reverse transcription was performed with 2 µg of isolated RNA, 500 ng oligo(dT)15 primer, 40 U of RNasin, 0.5 mM dNTPs, and 20 U of M-MLV-Reverse Transcriptase (Promega). Total RNA was DNase treated prior to reverse transcription to remove genomic DNA. Reverse transcription reactions were verified by *β-actin* RT-PCR using cDNA amplified with GoTaq Flexi (Promega). qPCR was performed using SYBR Green GoTaq qPCR master mix (Promega) according to manufacturer's instructions on LightCycler 96 SW 1.0 (Roche). Primer sequences have been supplied (Table 6). Reactions were performed on cDNA equivalent to 50 ng of total RNA and carried out for 45 amplification cycles. SYBR® Green fluorescence was measured after the extension step at the end of each amplification cycle and quantified using LightCycler Analysis Software (Roche). For each sample, a replicate omitting the reverse transcription step was undertaken as a negative control. qPCR data was normalized to the house-keeping control *Cyclophilin.* Experiments were replicated at least 3 times prior to statistical assessment. Each PCR was performed on at least 3 separate cell isolations, of which a representative PCR or an average is shown (ESI†).

Table 6. Primer sequences used in qPCR assay.

Human gene	Forward Sequence (5'-3')	Reverse Sequence (5'-3')	Annealing Temp (ºC)
Gli2	ATCTCTTGCCACC ATTCCAT	GGACAGAATGAG GCTCGTAA	60
SMO	CTGCCACTTCTAC GACTTCT	GGCCTGACATAGC ACATAGT	56
SuFu	GACCCCTTGGACT ATGTTAG	CTGATGTAGTGCC AGTGCTC	55
Ptch1	CCCTCACGTCCAT CAGCAAT	AACACCACTACTA CCGCTGC	58
Mouse gene			
Gli2	TCCAGTCAATGGT TCTGTCC	TGGCTCAGCATCG TCACTTC	60
Gli3	GGCCGTTACCATT ATGATCC	CTGAGGCTGCAGT GGGATTA	60
Shh	TGCTTTGTAACCG CCACTTT	CGCTGCTAGGTGC ACTTTTA	61
SMO	GAACTCCAATCGC TACCCTG	ATCTGCTCGGCAA ACAATCT	60
SuFu	GACCCCTTGGACT ATGTTAG	CTGATGTAGTGCC AGTGCTC	55
Ptch1	CATAGCTGCCCAG TTCAAGT	GGTCGTAAAGTAG GTGCTGG	55

Statistical analysis

Statistical analysis was performed using F-test and t-test in Excel 2013. * P < .05, ** P < .001, *** P < .0001.

Chemistry

All reagents were purchased from Sigma-Aldrich, Matrix Scientific or Lancaster Synthesis and were used without purification. All solvents were re-distilled from glass prior to use.

^1H and ^{13}C NMR spectra were recorded on a Brüker Advance™ AMX 400 MHz spectrometer at 400.13 and 100.62 MHz, respectively. Chemical shifts (δ) are reported in parts per million (ppm) measured to relative the internal standards. Coupling constants (*J*) are expressed in hertz (Hz). Mass spectra were recorded on a Shimadzu LCMS 2010 EV using a mobile phase of 1 : 1 acetonitrile–H_2O with 0.1% formic acid. High resolution mass spectra (HRMS) were determined using nanoflow reversed phased Liquid Chromatography (Dionex Ultimate 3000 RSLCnano, Thermo Fischer Scientific) coupled directly to a High Resolution mode equipped, Q-Exactive Plus

Hybrid Quadrupole-Orbitrap Mass Spectrometer (Thermo Fischer Scientific). This system was fitted with 5µm C18 nanoViper trap column (100um x 2cm, Acclaim PepMap100, Thermo) for desalting and pre-concentration, and separation was then performed at 300nl/min over an EASY-Spray PepMap column (3um C18, 75um x 15cm) utilising a gradient of 2-99% Buffer B (80% Acetonitrile, 0.1% Formic Acid) over 25 minutes.

Analytical HPLC traces were obtained using a Shimadzu system possessing a SIL-20A auto-sampler, dual LC-20AP pumps, CBM-20A bus module, CTO-20A column heater, and a SPD-20A UV/vis detector. This system was fitted with an Alltima™ C18 5 µm 150 mm × 4.6 mm column with solvent A: 0.06% Trifluoroacetic acid (TFA) in water and solvent B: 0.06% TFA in CH_3CN–H_2O (90 : 10). In each case HPLC traces were acquired at a flow rate of 2.0 mL min^{-1}, gradient 10–100 (%B), over 15.0 min, with detection at 220 nm and 254 nm.

Melting points were recorded on a Büchi Melting Point M-565. IR spectra were recorded on a PerkinElmer Spectrum Two™ FTIR Spectrometer with the UATR accessories. Thin layer chromatography (TLC) was performed on Merck 60 F254 pre-coated aluminium plates with a thickness of 0.2 mm. Column chromatography was performed under 'flash' conditions on Merck silica gel 60 (230–400 mesh).

Experimental data

Compounds **5** and **10**-**19** were prepared as described in ref 48. The relative configuration for the obtained products was assigned computationally as follow: Each of the initial geometry of each analogue (**14**-**16**) was built using the molecular builder of Molecular Operating Environment (MOE). Each molecule was relaxed using the semi-empirical AM1 method in MOE with a root mean square (rms) gradient of 0.01. Each analogue was subjected to conformational analysis using Stochastic Conformational Search method. The most stable conformation for each analogue was retained and saved as a mol2 file format. Each conformer was subjected to geometry optimization at DFT level of theory using B3LYP function with the 6-31+G(d,p) basis set. At this stage the DFT energy was calculated. The optimized structures were used for the calculation of NMR chemical shifts (relative to TMS) using the GIAO (gauge-independent (or including) atomic orbitals) method and the B3LYP functional with the 6-311+G(2d,p) basis set. The calculated DFT energy and ^{1}HNMR chemical shifts for selected peaks were used for assigning the configuration for the major and minor isomeric products (ESI, Table S1).

*2-(3-Cyano-2-oxo-4-methylquinolin-1(2H)-yl)-2-(1-methyl-1H-indol-3-yl)-N-(pentan-2-yl)acetamide (**20**)*

General procedure: A solution of MeOH (5.0 mL), 2-aminoacetophenone (0.148 mL, 1.23 mmol) and 1-methyl-1*H*-indole-3-carboxaldehyde (0.196 g, 1.23 mmol) was stirred at room temperature for 0.5 h. To the stirred solution was added cyanoacetic acid (0.105 g, 1.23 mmol) followed by the addition of 2-pentylisocyanide (0.152 mL, 1.23 mmol). The reaction mixture was stirred at room temperature for 24 h and the crude material was subjected to silica gel column chromatography (1:4 hexanes–EtOAc) to afford **4** (70 mg, 13%) as an off white solid (mp 243-245°C).

IR (cm^{-1}): 3246 (NH), 3083 (CH), 2972 (CH), 2229 (CN), 1637 (CO); The ^{1}H NMR displays a mixture of isomers, with the ratio 1.35 : 1.0 calculated at 0.74 and 0.60 ppm, respectively. ^{1}H is reported as a whole without splitting due to the complex overlapping. All peaks detected in ^{13}C are reported. ^{1}H NMR (400 MHz, DMSO-d_6) δ 7.91 (d, *J* = 8.2 Hz, 1H), 7.83 – 7.69 (m, 2H), 7.67 – 7.51 (m, 2H), 7.47 – 7.35 (m, 3H), 7.29 (dd, *J* = 9.8, 5.4 Hz, 1H), 7.13 (t, *J* = 7.6 Hz, 1H), 7.01 (t, *J* = 7.4 Hz, 1H), 3.98-3.86 (m, 1H), 3.75 (s, 3H), 2.75 (d, *J* = 3.2 Hz, 3H), 1.54 – 1.15 (m, 4H), 0.93-0.87 (m, 3H), 0.77-0.56 (m, 2H); ^{13}C NMR (101 MHz, DMSO-d_6) δ 167.4, 166.8, 159.2, 159.2, 158.3, 158.3, 139.1, 136.6, 136.5, 133.3, 133.2, 130.9, 130.81, 127.7, 127.6, 127.6, 123.4, 121.9, 120.1, 120.1, 119. 8, 118.9, 118.1, 118.1, 116.2, 110.4, 107.7, 106.2, 106.1, 106.1, 60.2, 53.8, 53.7, 52.9, 45.3, 45.2, 38.3, 38.0, 33.0 (Cx2), 27.4, 26.8, 21.2, 21.1, 20.8, 19.6, 19.1, 18.8, 14.6, 14.3, 14.2, 11.2, 10.8; LRMS (ESI-) m/z 440, 520 $[M+DMSO+2H]^+$ 100%. HRMS (ES+) for $C_{27}H_{28}N_4O_2Na$; calculated 463.2110, found 463.2104; RP-HPLC Alltima™ C18 5 µm 150 mm x 4.6 mm, 10–100% B in 15 min, R_t min = 7.07, 93 %.

*2-(3-Cyano-2-oxo-4-phenylquinolin-1(2H)-yl)-2-(1H-indol-3-yl)-N-(pentan-2-yl)acetamide (**21**)*

Synthesized utilizing the general procedure described above, from 2-aminobenzophenone (0.252 g, 1.28 mmol), indole-3-carboxaldehyde (0.186g, 1.28 mmol), cyanoacetic acid (0.109 g, 1.28 mmol) and 2-pentylisocyanide (0.158 mL, 1.28 mmol) in MeOH (5.0 mL) to afford **6** (0.07 g, 11%) as an off white solid (mp 182–183 ºC).

IR (cm^{-1}): 3420 (NH), 2229 (CN), 1678 (CONH), 1646 (CON); The ^{1}H NMR displays a mixture of isomers, with the ratio 5.5 : 1.0 calculated at 3.96 and 3.72 ppm, respectively. ^{1}H is reported as a whole without splitting due to the complex overlapping. All peaks detected in ^{13}C are reported ^{1}H NMR (400 MHz, DMSO-*d6*) δ 11.26 (s, 1H), 7.85 (s, 2H), 7.73 – 7.32 (m, 10H), 7.29 – 6.87 (m, 4H), 3.96 (s, 1H), 1.84 – 0.09 (m, 11H); ^{13}C NMR (101 MHz, DMSO) δ 167.4, 166.8, 160.1, 159.3, 140.1, 136.2, 136.1, 134.1, 133.3, 130.4, 129.3, 129.2, 129.1, 127.4, 127.3, 127.0, 126.9, 123.5, 122.0, 119.9, 119.8, 118.8, 118.6, 116.0, 112.2, 108.5, 106.0, 54.3, 54.2, 53.0, 45.4, 45.3, 38.4, 38.2, 27.4, 26.9, 21.1, 20.9, 19.6, 19.2, 14.4, 14.2, 11.3, 10.8; LRMS (ESI+) m/z 488, 489 $[M+H]^+$, 40%. HRMS (ES+) for $C_{31}H_{28}N_4O_2$; calculated 489.2285, found 489.2284; RP-HPLC Phenomenex Onyx™ Monolithic C18 5 µm 100 mm x 4 mm, 10–100% B in 15 min, R_t min = 12.24, 100 %.

*2-(3-Cyano-2-oxo-4-phenylquinolin-1(2H)-yl)-2-(1H-indol-5-yl)-N-(pentan-2-yl)acetamide (**22**)*

Synthesized utilizing the general procedure described above, from 2-aminobenzophenone (0.267 g, 1.35 mmol), indole-5-carboxaldehyde (0.197g, 1.35 mmol), cyanoacetic acid (0.115 g, 1.35 mmol) and 2-pentylisocyanide (0.167 mL, 1.35 mmol) in MeOH (5.0 mL) to afford **6** (0.238 g, 36%) as an off white solid (mp 271–272 ºC).

IR (cm^{-1}): 3403 (NH), 3338 (NH), 2956 (CH), 2235(CN), 1647 (CO); The ^{1}H NMR displays a mixture of isomers, with the ratio

2.45 : 1.0 calculated at 0.74 and 0.64 ppm, respectively. ^{1}H is reported as a whole without splitting due to the complex overlapping. All peaks detected in ^{13}C are reported ^{1}H NMR (400 MHz, DMSO-d_6) δ 11.13 (s, 1H), 7.89 (dd, *J* = 14.3, 8.1 Hz, 1H), 7.71 – 7.52 (m, 7H), 7.52 – 7.44 (m, 1H), 7.41 – 7.29 (m, 2H), 7.26 – 7.01 (m, 4H), 6.40 (d, *J* = 1.8 Hz, 1H), 3.91 (dd, *J* = 13.4, 7.0 Hz, 1H), 1.59 – 1.19 (m, 3H), 1.16 – 0.99 (m, 2H), 0.99 – 0.84 (m, 3H), 0.81-0.55 (m, 2H);

^{13}C NMR (101 MHz, DMSO-d_6) δ 167.5, 167.0, 166.9, 160.1, 160.0, 159.4, 140.6, 135.6, 134.2, 134.2, 133.1, 133.0, 130.4, 129.3 (Cx2), 129.2 (Cx2), 129.1, 129.1, 128.0, 126.5, 126.5, 125.8, 125.7, 125.6, 123.5, 121.8, 120.1, 120.1, 120.0, 119.1, 119.0, 116.0, 116.0, 111.9, 111.9, 106.3, 106.3, 106.2, 101.8, 101.7, 61.3, 61.1, 61.1, 52.8, 45.3, 45.2, 38.3, 38.2, 27.2, 26.8, 21.2, 20.9, 19.5, 19.0, 14.4, 14.3, 11.1, 10.6; LRMS (ESI-) m/z -488, 520 [M+CH_3OH-H] 95%. HRMS (ES+) for $C_{31}H_{28}N_4O_2$; calculated 489.2285, found 489.2284.

RP-HPLC Alltima™ C18 5 µm 150 mm x 4.6 mm, 10–100% B in 15 min, R_t min = 7.07, >98 %.

*2-(3-Cyano-2-oxo-4-phenylquinolin-1(2H)-yl)-2-(5-methyl-1H-indole-3-yl)-N-(pentan-2-yl) acetamide (**23**)*

Synthesized utilizing the general procedure described above, from 2-aminobenzophenone (0.378 g, 1.92 mmol), 5-methyl-1*H*-indole carbaldehyde (0.305 g, 1.92 mmol), cyanoacetic acid (0.163 g, 1.92 mmol), and 2-pentylisocyanide (0.237 mL, 1.92 mmol) to afford **23** (0.445 g, 46%) as an off white solid (mp 178–180 ºC).

IR (cm^{-1}): 3427 (br NH), 2962(CH), 2236 (CN), 1645(CON); The ^{1}H NMR displays a mixture of isomers, with the ratio 2.1 : 1.0 calculated at 0.77 and 0.68 ppm, respectively. ^{1}H is reported as a whole without splitting due to the complex overlapping. All peaks detected in ^{13}C are reported ^{1}H NMR (400 MHz, DMSO-d_6) δ 11.13 (d, *J* = 4.9 Hz, 1H), 7.90 – 7.37 (m, 10H), 7.29-7.16 (m, 4H), 6.92 (d, *J* = 8.3 Hz, 1H), 4.03 – 3.87 (m, 1H), 2.34 (s, 3H), 1.57 – 1.20 (m, 3H), 1.20 – 0.86 (m, 5H), 0.82-0.60 (m, 3H); ^{13}C NMR (101 MHz, DMSO-d_6) δ 167.5, 166.9, 160.1, 160.1, 159.3, 140.1, 140.1, 134.6, 134.6, 134.5, 134.1, 133.3, 130.4, 129.4, 129.2, 129.1, 128.2, 128.1, 127.5, 127.5, 126.8, 126.6, 123.5, 119.9, 118.5, 118.4, 118.3, 116.0, 111.9, 107.9, 107.9, 106.0, 105.9, 54.5, 54.4, 52.9, 45.4, 45.2, 38.4, 38.2, 27.3, 26.9, 21.9, 21.1, 20.9, 19.6, 19.2, 14.4, 14.2, 11.2, 10.8; LRMS (ESI-) m/z 502, 521 [M+NH_4]$^{+}$ 40%. HRMS (ES+) for $C_{32}H_{30}N_4O_2$; calculated 503.2442, found 503.2444; RP-HPLC Alltima™ C18 5 µm 150 mm x 4.6 mm, 10–100% B in 15 min, R_t min = 10.89, 100%.

*Ethyl-[2-(3-Cyano-2-oxo-4-phenyl-2H-quinolin-1-yl)-2-(5-methyl-1H-indol-3-yl)-acetamido]-acetate (**24**)*

Synthesized utilizing the general procedure described above, from 2-aminobenzophenone (0.390 g, 1.98 mmol), 5-methyl-indole-3-carboxaldehyde (0.315g, 1.98 mmol), cyanoacetic acid (0.168 g, 1.98 mmol) and ethyl isocyanoacetate (0.216 mL, 1.98 mmol) in MeOH (5.0 mL) to afford **9** (0.347 g, 34%) as a greenish solid (mp 199-200 °C).

IR (cm^{-1}): 3423 (NH), 3410 (NH), 2232 (CN), 1731 (COO), 1673 (CON); ^{1}H NMR (400 MHz, DMSO-d_6) δ 11.21 (d, *J* = *1*.8 Hz, 1H), 8.53 (s, 1H), 7.83 (d, *J* = 8.7 Hz, 1H), 7.72 – 7.48 (m, 8H), 7.32 – 7.17 (m, 4H), 6.92 (d, *J* = 8.3 Hz, 1H), 4.14 (q, *J* = 7.1 Hz, 2H), 4.02-3.84 (m, 2H), 2.34 (s, 3H), 1.22 (t, *J* = 7.1 Hz, 3H); ^{13}C NMR (101 MHz, DMSO-d_6) δ 170.2, 168.4, 160.3, 159.3, 139.7, 134.5, 134.1, 133.5, 130.5, 129.4, 129.4, 129.4, 129.1, 129.0, 128.3, 127.5, 127.1, 123.7 (Cx2), 119.9, 118.5, 118.2, 115.8, 111.9, 107.3, 105.8, 61.0, 53.8, 41.9, 21.9, 14.6; LRMS (ESI+) m/z518, 541 [M+Na-H]$^{+}$ 60%. HRMS (ES+) for $C_{31}H_{26}N_4O_4$; calculated 519.2027, found 519.2026; RP-HPLC Alltima™ C18 5 µm 150 mm x 4.6 mm, 10–100% B in 15 min, R_t min = 13.72, >97%.

*Ethyl-[2-(3-Cyano-2-oxo-4-phenyl-2H-quinolin-1-yl)-2-(1H-indol-3-yl)-acetamido]-acetate (**25**)*

Synthesized utilizing the general procedure described above, from 2-aminobenzophenone (0.366 g, 1.86 mmol), 1*H*-indole carbaldehyde (0.269 g, 1.86 mmol), cyanoacetic acid (0.157 g, 1.86 mmol), and ethyl isocyanoacetate (0.202 mL, 1.86 mmol) to afford **25** (0.30 g, 46%) as an off white solid (mp 179.3-180.5 °C).

IR (cm^{-1}): 3420 (NH), 2236 (CN), 1737 (COO), 1686 (CONH), 1646 (CON); ^{1}H NMR (400 MHz, DMSO-*d6*) δ 11.35 (s, 1H), 8.58 (s, 1H), 7.93 – 7.75 (m, 2H), 7.75-7.45 (m, 8H), 7.39 (d, J = 8.0 Hz, 1H), 7.21 (d, J = 3.7 Hz, 2H), 7.15-6.91 (m, 2H), 4.25 – 4.06 (m, 2H), 4.04-3.80 (m, 2H), 1.22 (t, J = 7.0 Hz, 3H); ^{13}C NMR (101 MHz, DMSO-d_6) δ 170.2, 168.4, 160.3, 159.3, 139.7, 136.1, 134.0, 133.5, 130.5, 129.5, 129.4 (Cx2), 129.3 (Cx2), 129.2, 129.0, 127.3, 123.7, 122.1, 120.0 (Cx2), 118.6, 118.5, 115.9, 112.2, 107.8, 105.8, 61.1, 53.7 41.9, 14.6; LRMS (ESI+) m/z 504, 505 [M+H]$^{+}$, 100%. HRMS (ES+) for $C_{30}H_{24}N_4O_4$; calculated 505.1870, found 505.1869; RP-HPLC Phenomenex Onyx™ Monolithic C18 5 µm 100 mm x 4 mm, 10–100% B in 15 min, R_t min = 11.09, 100%.

*Ethyl-[2-(3-Cyano-2-oxo-4-phenyl-2H-quinolin-1-yl)-2-(1-methylindole-3-yl)-acetamido]-acetate (**26**)*

Synthesized utilizing the general procedure described above, from 2-aminobenzophenone (0.281 g, 1.43 mmol), 1-methyl-indole-3-carboxaldehyde (0.227 g, 1.43 mmol), cyanoacetic acid (0.121 g, 1.43 mmol) and ethyl isocyanoacetate (0.156 mL, 1.43 mmol) in MeOH (5.0 mL). The crude material was subjected to silica gel column chromatography (1:1 hexanes–EtOAc) to afford **26** (0.192 g, 26%) as an off white solid (mp 209-211°C).

IR (cm^{-1}): 3422 (NH), 2920 (CH), 2229 (CN), 1743 (COO), 1639 (CON); ^{1}H NMR (400 MHz, DMSO-d_6) δ 8.53 (bs, 1H), 7.85 (d, *J* = 8.8 Hz, 1H), 7.75 (s, 1H), 7.70 – 7.48 (m, 7H), 7.43 (d, *J* = 8.2 Hz, 1H), 7.25 – 7.19 (m, 2H), 7.17 (t, *J* = 7.2 Hz, 1H), 7.06 (t, *J* = 7.2 Hz, 1H),, 4.12 (q, *J* = 7.1 Hz, 2H), 3.90 (d, *J* = 6.6 Hz, 2H), 3.79 (s, 3H), 1.20 (t, *J* = 7.1 Hz, 3H); ^{13}C NMR (101 MHz, DMSO-d_6) δ 170.1, 168.3, 160.3, 159.2, 139.6, 136.5, 134.0, 133.7, 131.4, 130.5, 129.5, 129.4 (Cx2), 129.2, 129.0, 127.7, 123.7, 122.1, 120.1, 120.0, 118.9, 118.2, 115.9, 110.5, 106.8, 105.9, 105.9, 61.0, 41.9, 33.2, 14.6; LRMS (ESI-) m/z 518, 540 [M+ Na-H]$^{+}$, 100%. HRMS (ES+) for $C_{31}H_{26}N_4O_4$; calculated 519.2027, found 519.2027; RP-HPLC Alltima™ C18 5 µm 150 mm x 4.6 mm, 10–100% B in 15 min, R_t min = 14.26, >98%.

*Ethyl-3-[2-(3-cyano-2-oxo-4-phenyl-2H-quinolin-1-yl)-2-(1-methyl-1H-indol-3-yl)-acetylamino]-propionate (**27**)*

Synthesized utilizing the general procedure described above, from 2-aminobenzophenone (0.186 g, 0.94 mmol), 1-methyl-indole-3-carboxaldehyde (0.15g, 0.94 mmol), cyanoacetic acid (0.08 g, 0.94 mmol) and ethyl isocyanopropionate (0.12 mL, 0.94 mmol) in MeOH (5.0 mL) to afford **27** (0.149 g, 50%) as a white solid (mp 267-268°C).

IR (cm^{-1}): 3410 (NH), 2232 (CN), 1725 (COO), 1686 (CON); ^{1}H NMR (400 MHz, DMSO-d_6) δ 8.05 (bs, 1H), 7.83 (d, J = 8.7 Hz, 1H), 7.71 – 7.56 (m, 6H), 7.56 – 7.47 (m, 2H), 7.45-7.38 (m, 2H), 7.26 – 7.20 (m, 2H), 7.17 (t, J = 7.2 Hz, 1H), 7.06 (t, J = 7.2 Hz, 1H), 4.03 (q, J = 7.1 Hz, 2H), 3.78 (s, 3H), 3.42 – 3.35 (m, 2H), 2.57-2.44 (m, 2H), 1.16 (t, J = 7.1 Hz, 3H); ^{13}C NMR (101 MHz, DMSO-d_6) δ 171.7, 167.7, 160.1, 159.0, 139.9, 136.5, 134.1, 133.8, 131.3, 130.5, 129.6, 129.4, 129.2, 129.0, 127.8, 123. 7, 122.1, 120.0, 119.9, 119.0, 117.8, 115.9, 110. 5, 107.1, 106.1, 60.4, 54.1, 35.9, 34.0, 33.1, 14.5; LRMS (ESI+) m/z 532, 287 $[M+ACN+ 2H]^{2+}$ 100%. HRMS (ES+) for $C_{16}H_{11}N_2O^+$ (main fragment); calculated 247.087, found 247.0865; RP-HPLC Alltima™ C18 5 µm 150 mm x 4.6 mm, 10–100% B in 15 min, R_t min = 14.46, >95%.

*Ethyl-2-(2-(5-chloro- indole (1H)-3-yl)-2-(3-cyano-2-oxo-4-phenyl-1(2H)-quinolin-yl)-acetamido)-acetate (**28**)*

Synthesized utilizing the general procedure described above, from 2-aminobenzophenone (0.478 g, 2.4 mmol), 5-chloro-indole-3-carboxaldehyde (0.434g, 2.4 mmol), cyanoacetic acid (0.204 g, 2.4 mmol) and ethyl isocyanoacetate (0.271 mL, 2.4 mmol) in MeOH (5.0 mL) to afford **28** (0.435 g, 33%) as a yellowish precipitate (mp 201–203°C).

IR (cm^{-1}): 3415 (NH), 3406 (NH), 2236(CN), 1736(COO), 1671(CON); ^{1}H NMR (400 MHz, DMSO-d_6) (Isomeric mixture) δ 11.54 (d, *J* = 1.4 Hz, 1H), 8.53 (s, 1H), 7.82 (dd, *J* = 11.9, 5.5 Hz, 2H), 7.71 – 7.61 (m, 4H), 7.61-7.5 (m, 4H), 7.42 (d, *J* = 8.6 Hz, 1H), 7.29 – 7.18 (m, 2H), 7.12 (dd, *J* = 8.6, 1.7 Hz, 1H), 4.14 (q, *J* = 7.0 Hz, 2H), 3.93 (qd, *J* = 17.2, 5.8 Hz, 2H), 1.22 (t, *J* = 7.1 Hz, 3H); ^{13}C NMR (101 MHz, DMSO-d_6) δ 170.1, 168.2, 160.4, 159.2, 139.6, 134.6, 134.0, 133.7, 130.5, 129.6(Cx2), 129.4, 129.2, 129.0 (Cx2), 128.5, 124.5, 123.8, 122.0, 120.1, 118.3 (Cx2), 118.2, 115.8, 113.8, 107.8, 106.0, 61.0, 42.0, 14.6; LRMS (ESI+) m/z 538, 292 $[M+2Na]^{2+}$, 60%. HRMS for $C_{30}H_{23}ClN_4O_4$; calculated 539.1481, found 539.1481; RP-HPLC Alltima™ C18 5 µm 150 mm x 4.6 mm, 10–100% B in 15 min, R_t min = 14.07, >99%.

*N-tert-Butyl-2-(3-cyano-2-oxo-4-phenyl-2H-quinolin-1-yl)-2-(5-methyl-1H-indol-3-yl)-acetamide (**29**)*

Synthesized utilizing the general procedure described above, from 2-aminobenzophenone (0.359 g, 1.83 mmol), 5-methyl-indole-3-carboxaldehyde (0.290g, 1.83 mmol), cyanoacetic acid (0.156 g, 1.83 mmol) and *tert*-butyl isocyanide (0.207 mL, 1.83 mmol) in MeOH (5.0 mL) to afford **29** (0.419g, 47%) as a white solid (mp 196-198°C).

IR (cm^{-1}): 3427(NH), 2978 (CH), 2228 (CN), 1650 (CON); ^{1}H NMR (400 MHz, DMSO-*d6*) (Isomeric mixture) δ 11.13 (d, J = 4.9 Hz, 1H), 7.90 – 7.37 (m, 10H), 7.29-7.16 (m, 4H), 6.92 (d, J = 8.3 Hz, 1H), 4.03 – 3.87 (m, 1H), 2.34 (s, 3H), 1.57 – 1.20 (m, 3H), 1.20 –0.86 (m, 5H), 0.82-0.60 (m, 3H); ^{13}C NMR (101 MHz, DMSO) (Isomeric mixture) δ 167.5, 166.9, 160.1, 160.1, 159.3, 140.1, 140.1, 134.6, 134.6, 134.5, 134.1, 133.3, 130.4, 129.4, 129.2, 129.1, 128.2, 128.1, 127.5, 127.5, 126.8, 126.6, 23.5, 19.9, 118.48, 118.4, 118.3, 116.0, 111.9, 107.9, 107.9, 106.0, 105.9, 54.5, 54.4, 52.9, 45.4, 45.2, 38.4, 38.2, 27.3, 26.9, 21.9, 21.1, 20.9, 19.6, 19.2, 14.4, 14.2, 11.2, 10.8; LRMS (ESI-) m/z 488, 243 $[M-2H]^{2+}$, 90%. HRMS for $C_{31}H_{28}N_4O_2$; calculated 489.2285, found 489.2283; RP-HPLC Alltima™ C18 5µµm 150 mm x 4.6 mm, 10–100% B in 15 min, R_t min = 14.59, >95%.

*N-tert-Butyl-2-(3-cyano-2-oxo-4-phenyl-2H-quinolin-1-yl)-2-(1-methyl-1H-indole-3-yl)-acetamide (**30**)*

Synthesized utilizing the general procedure described above, from 2-aminobenzophenone (0.311 g, 1.58 mmol), 1-methyl-indole-3-carboxaldehyde (0.251g, 1.58 mmol), cyanoacetic acid (0.134 g, 1.58 mmol) and *tert*-butyl isocyanide (0.178 mL, 1.58 mmol) in MeOH (5.0 mL) to afford **29** (0.200 g, 26%) as a white solid (mp 232-234°C).

IR (cm^{-1}): 3357 (NH), 2979 (CH), 2229 (CN), 1650 (CO); ^{1}H NMR (400 MHz, DMSO) δ 7.89 (d, J = 8.8 Hz, 1H), 7.68 – 7.46 (m, 9H), 7.43 (d, J = 7.8 Hz, 2H), 7.22-7.13 (m, 3H), 7.06 (t, J = 7.4 Hz, 1H), 3.79 (s, 3H), 1.32 (s, 9H); ^{13}C NMR (101MHz, DMSO) δ 166.66, 160.13, 159.17, 140.28, 136.75, 134.09, 133.34, 130.54, 130.42, 129.31 (Cx3), 129.15 (Cx2), 127.48, 123.52, 122.17, 119.99, 119.78, 119.04, 118.55, 115.91, 110.53, 108.04, 105.89, 54.94, 51.57, 33.09, 28.83 (Cx3); LRMS (ESI+) m/z 488, 243 $[M-2H]^{2+}$, 100%. HRMS (ES+) for $C_{31}H_{28}N_4O_2$; calculated 489.2285, found 489.2287; RP-HPLC Alltima™ C18 5µm 150 mm x 4.6 mm, 10–100% B in 15 min, R_t min =7.03, 96%

More information on the synthesis and characterization of the analogues can be found in the ESI.

Acknowledgements

The authors thank the NHMRC (Australia) for project support, Nathan Druery Smith (Analytical and Biomolecular Research Facility at the University of Newcastle) for the HRMS data, James K. Chen for helpful discussions and T.N.T. is the recipient of a Prime Minister's Australia Asia Postgraduate Endeavour Award.

Notes and References

1 A. P. McMahon, P. W. Ingham and C. J. Tabin, *Curr. Top. Develop. Biol.*, 2003, **53**, 1-114.
2 P. W. Ingham, *Genes Dev.*, 2001, **15**, 3059-3087.
3 E. H. Epstein, *Nat. Rev. Cancer*, 2008, **8**, 743-754.
4 C. Raffel, R. B. Jenkins, L. Frederick, D. Hebrink, B. Alderete, D. W. Fults and C. D. James, *Cancer Res.*, 1997, **57**, 842-845.
5 T. Pietsch, A. Waha, A. Koch, J. Kraus, S. Albrecht, J. Tonn, N. Sorensen, F. Berthold, B. Henk, N. Schmandt, H. K. Wolf, A. von Deimling, B. Wainwright, G. Chenevix-Trench, O. D. Wiestler and C. Wicking, *Cancer Res.*, 1997, **57**, 2085-2088.
6 D. G. Evans, P. A. Farndon, L. D. Burnell, H. R. Gattamaneni and J. M. Birch, *Br. J. Cancer*, 1991, **64**, 959-961.
7 S. P. Thayer, M. Pasca di Magliano, P. W. Heiser, C. M. Nielsen, D. J. Roberts, G. Y. Lauwers, Y. P. Qi, S. Gysin, C. Fernandez-del Castillo, V. Yajnik, B. Antoniu, M. McMahon, A. L. Warshaw and M. Hebrok, *Nature*, 2003, **425**, 851-856.

8 S. Karhadkar Sunil, G. S. Bova, N. Abdallah, S. Dhara, D. Gardner, A. Maitra, T. Isaacs John, M. Berman David and A. Beachy Philip, *Nature*, 2004, **431**, 707-712.
9 Z. Yuan, J. A. Goetz, S. Singh, S. K. Ogden, W. J. Petty, C. C. Black, V. A. Memoli, E. Dmitrovsky and D. J. Robbins, *Oncogene*, 2007, **26**, 1046-1055.
10 D. N. Watkins, M. Berman David, G. Burkholder Scott, B. Wang, A. Beachy Philip and B. Baylin Stephen, *Nature*, 2003, **422**, 313-317.
11 D. Qualtrough, A. Buda, W. Gaffield, C. Williams Ann and C. Paraskeva, *Int. J. Cancer*, 2004, **110**, 831-837.
12 D. M. Berman, S. S. Karhadkar, A. Maitra, R. Montes De Oca, M. R. Gerstenblith, K. Briggs, A. R. Parker, Y. Shimada, J. R. Eshleman, D. N. Watkins and P. A. Beachy, *Nature*, 2003, **425**, 846-851.
13 M. Kasper, V. Jaks, M. Fiaschi and R. Toftgaard, *Carcinogenesis*, 2009, **30**, 903-911.
14 S. Mukherjee, N. Frolova, A. Sadlonova, Z. Novak, A. Steg, G. P. Page, D. R. Welch, S. M. Lobo-Ruppert, J. M. Ruppert, M. R. Johnson and A. R. Frost, *Cancer Biol. Ther.*, 2006, **5**, 674-683.
15 X. Chen, A. Horiuchi, N. Kikuchi, R. Osada, J. Yoshida, T. Shiozawa and I. Konishi, *Cancer Sci.*, 2007, **98**, 68-76.
16 M. Zbinden, A. Duquet, A. Lorente-Trigos, S.-N. Ngwabyt, I. Borges and A. Ruiz i Altaba, *Embo J.*, 2010, **29**, 2659-2674.
17 A. Po, E. Ferretti, E. Miele, E. De Smaele, A. Paganelli, G. Canettieri, S. Coni, L. Di Marcotullio, M. Biffoni, L. Massimi, C. Di Rocco, I. Screpanti and A. Gulino, *Embo J.*, 2010, **29**, 2646-2658.
18 FDA approves new treatment for most common form of advanced skin cancer, http://www.fda.gov/NewsEvents/Newsroom/PressAnnouncements/ucm455862.htm).
19 FDA approves new treatment for most common type of skin cancer http://www.fda.gov/NewsEvents/Newsroom/PressAnnouncements/ucm289545.htm).
20 T. N. Trinh, E. A. McLaughlin, C. P. Gordon and A. McCluskey, *MedChemComm*, 2014, **5**, 117-133.
21 R. Nanta, D. Kumar, D. Meeker, M. Rodova, P. J. Van Veldhuizen, S. Shankar and R. K. Srivastava, *Oncogenesis*, 2013, **2**, e42. doi: 10.1038/oncsis.2013.5.
22 J. K. Chen, J. Taipale, K. E. Young, T. Maiti and P. A. Beachy, *Proc. Nat. Acad. Sci., USA,* 2002, **99**, 14071-14076.
23 R. Maun Henry, X. Wen, A. Lingel, J. de Sauvage Frederic, A. Lazarus Robert, J. Scales Suzie and G. Hymowitz Sarah, *J. Biol. Chem.*, 2010, **285**, 26570-26580.
24 B. Z. Stanton, L. F. Peng, N. Maloof, K. Nakai, X. Wang, J. L. Duffner, K. M. Taveras, J. M. Hyman, S. W. Lee, A. N. Koehler, J. K. Chen, J. L. Fox, A. Mandinova and S. L. Schreiber, *Nat. Chem. Biol.*, 2009, **5**, 154-156.
25 J. Kim, B. T. Aftab, J. Y. Tang, D. Kim, A. H. Lee, M. Rezaee, J. Kim, B. Chen, E. M. King, A. Borodovsky, G. J. Riggins, E. H. Epstein, P. A. Beachy and C. M. Rudin, *Cancer Cell*, 2013, **23**, 23-34.
26 A. Solinas, H. Faure, H. Roudaut, E. Traiffort, A. Schoenfelder, A. Mann, F. Manetti, M. Taddei and M. Ruat, *J. Med. Chem.*, 2012, **55**, 1559-1571.
27 T. Ohashi, Y. Oguro, T. Tanaka, Z. Shiokawa, Y. Tanaka, S. Shibata, Y. Sato, H. Yamakawa, H. Hattori, Y. Yamamoto, S. Kondo, M. Miyamoto, M. Nishihara, Y. Ishimura, H. Tojo, A. Baba and S. Sasaki, *Bioorg. Med. Chem.*, 2012, **20**, 5507-5517.
28 M. J. Munchhof, Q. Li, A. Shavnya, G. V. Borzillo, T. L. Boyden, C. S. Jones, S. D. LaGreca, L. Martinez-Alsina, N. Patel, K. Pelletier, L. A. Reiter, M. D. Robbins and G. T. Tkalcevic, *ACS Med. Chem. Lett.*, 2012, **3**, 106-111.
29 S. Pan, X. Wu, J. Jiang, W. Gao, Y. Wan, D. Cheng, D. Han, J. Liu, N. P. Englund, Y. Wang, S. Peukert, K. Miller-Moslin, J. Yuan, R. Guo, M. Matsumoto, A. Vattay, Y. Jiang, J. Tsao, F. Sun, A. C. Pferdekamper, S. Dodd, T. Tuntland, W. Maniara, J. F. Kelleher, III, Y.-m. Yao, M. Warmuth, J. Williams and M. Dorsch, *ACS Med. Chem. Lett.*, 2010, **1**, 130-134.
30 He, Biao; Fujii, Naoaki; MYou, Liang; Xu, Zhidong; Jablons, David M. *Dihydropyrazolecarboxamides and their preparation, pharmaceutical compositions and use in the targeting GLI proteins in human cancer by small molecules Application: WO Pat.,* 2009-GB50926 2010013037, 2010.
31 M. R. Tremblay, A. Lescarbeau, M. J. Grogan, E. Tan, G. Lin, B. C. Austad, L.-C. Yu, M. L. Behnke, S. J. Nair, M. Hagel, K. White, J. Conley, J. D. Manna, T. M. Alvarez-Diez, J. Hoyt, C. N. Woodward, J. R. Sydor, M. Pink, J. MacDougall, M. J. Campbell, J. Cushing, J. Ferguson, M. S. Curtis, K. McGovern, M. A. Read, V. J. Palombella, J. Adams and A. C. Castro, *J. Med. Chem.*, 2009, **52**, 4400-4418.
32 K. D. Robarge, S. A. Brunton, G. M. Castanedo, Y. Cui, M. S. Dina, R. Goldsmith, S. E. Gould, O. Guichert, J. L. Gunzner, J. Halladay, W. Jia, C. Khojasteh, M. F. T. Koehler, K. Kotkow, H. La, R. L. La Londe, K. Lau, L. Lee, D. Marshall, J. C. Marsters, L. J. Murray, C. Qian, L. L. Rubin, L. Salphati, M. S. Stanley, J. H. A. Stibbard, D. P. Sutherlin, S. Ubhayaker, S. Wang, S. Wong and M. Xie, *Bioorg. Med. Chem. Lett.*, 2009, **19**, 5576-5581.
33 M. R. Tremblay, M. Nevalainen, S. J. Nair, J. R. Porter, A. C. Castro, M. L. Behnke, L.-C. Yu, M. Hagel, K. White, K. Faia, L. Grenier, M. J. Campbell, J. Cushing, C. N. Woodward, J. Hoyt, M. A. Foley, M. A. Read, J. R. Sydor, J. K. Tong, V. J. Palombella, K. McGovern and J. Adams, *J. Med. Chem.*, 2008, **51**, 6646-6649.
34 V. Travaglione, C. Peacock, J. MacDougall, K. McGovern, J. Cushing, L. C. Yu, M. Trudeau, V. Palombella, J. Adams, J. Hierman, J. Rhodes, W. Devereux, and D.N. Watkins. *A novel HH pathway inhibitor, IPI-926, delays recurrence post-chemotherapy in a primary human SCLC xenograft model.* 99th AACR Annual Meeting. 2008. p. 4611.
35 M. Dai, F. He, R. K.Jain, R. Karki, J. F. Kelleher, J. Lei, L. Llamas, M. A. McEwan, K. Miller-Moslin, L. B. Perez, S. Peukert, and N. Yusuff. *Nitrogen-containing heterocyclic organic compounds as inhibitors of the hedgehog pathway and their preparation and use in the treatment of diseases. Application: WO Pat.,* 2008-EP53040 2008110611, 2008.
36 J. Fu, M. Rodova, S. K. Roy, J. Sharma, K. P. Singh, R. K. Srivastava and S. Shankar, *Cancer Lett.*, 2013, **330**, 22-32.
37 Y. Rifai, M. A. Arai, S. K. Sadhu, F. Ahmed and M. Ishibashi, *Bioorg. Med. Chem. Lett.*, 2011, **21**, 718-722.
38 T. Mazumdar, J. DeVecchio, T. Shi, J. Jones, A. Agyeman and J. A. Houghton, *Cancer Res.*, 2011, **71**, 1092-1102.
39 M. A. Arai, C. Tateno, T. Koyano, T. Kowithayakorn, S. Kawabe and M. Ishibashi, *Org. Biomol. Chem.*, 2011, **9**, 1133-1139.
40 M. Actis, M. C. Connelly, A. Mayasundari, C. Punchihewa and N. Fujii, *Biopolymers*, 2011, **95**, 24-30.
41 N. Mahindroo, M. C. Connelly, C. Punchihewa, L. Yang, B. Yan and N. Fujii, *Bioorg. Med. Chem.*, 2010, **18**, 4801-4811.
42 N. Mahindroo, C. Punchihewa and N. Fujii, *J. Med. Chem.*, 2009, **52**, 3829-3845.
43 J. M. Hyman, A. J. Firestone, V. M. Heine, Y. Zhao, C. A. Ocasio, K. Han, M. Sun, P. G. Rack, S. Sinha, J. J. Wu, D. E. Solow-Cordero, J. Jiang, D. H. Rowitch and J. K. Chen, *Proc. Nat. Acad. Sci. USA*, 2009, **106**, 14132-14137.
44 T. Hosoya, M. A. Arai, T. Koyano, T. Kowithayakorn and M. Ishibashi, *ChemBioChem*, 2008, **9**, 1082-1092.
45 M. A. Arai, C. Tateno, T. Hosoya, T. Koyano, T. Kowithayakorn and M. Ishibashi, *Bioorg. Med. Chem.*, 2008, **16**, 9420-9424.

46 M. Lauth, A. Bergstroem, T. Shimokawa and R. Toftgard, *Proc. Nat. Acad. Sci. USA*, 2007, **104**, 8455-8460.
47 T. N. Trinh, L. Hizartzidis, A. J. S. Lin, D. G. Harman, A. McCluskey and C. P. Gordon, *Org. Biomol. Chem.*, 2014, **12**, 9562-9571.
48 C. P. Gordon, K. A. Young, L. Hizartzidis, F. M. Deane and A. McCluskey, *Org. Biomol. Chem.*, 2011, **9**, 1419
49 H. Ajj, A. Chesnel, S. Pinel, F. Plenat, S. Flament and H. Dumond, *PLoS One*, 2013, **8**, e61758.
50 E. R. Cantwell-Dorris, J. J. O'Leary and O. M. Sheils, *Mol. Can. Therap.*, 2011, **10**, 385-394.
51 J. de Jong, H. Stoop, A. J. M. Gillis, R. Hersmus, R. J. H. L. M. van Gurp, G.-J. M. van de Geijn, E. van Drunen, H. B. Beverloo, D. T. Schneider, J. K. Sherlock, J. Baeten, S. Kitazawa, E. J. van Zoelen, K. van Roozendaal, J. W. Oosterhuis and L. H. J. Looijenga, *Genes, Chrom. Can.*, 2008, **47**, 185-196.
52 H. Davies, G. R. Bignell, C. Cox, P. Stephens, S. Edkins, S. Clegg, J. Teague, H. Woffendin, M. J. Garnett, W. Bottomley, N. Davis, E. Dicks, R. Ewing, Y. Floyd, K. Gray, S. Hall, R. Hawes, J. Hughes, V. Kosmidou, A. Menzies, C. Mould, A. Parker, C. Stevens, S. Watt, S. Hooper, R. Wilson, H. Jayatilake, B. A. Gusterson, C. Cooper, J. Shipley, D. Hargrave, K. Pritchard-Jones, N. Maitland, G. Chenevix-Trench, G. J. Riggins, D. D. Bigner, G. Palmieri, A. Cossu, A. Flanagan, A. Nicholson, J. W. C. Ho, S. Y. Leung, S. T. Yuen, B. L. Weber, H. F. Seigler, T. L. Darrow, H. Paterson, R. Marais, C. J. Marshall, R. Wooster, M. R. Stratton and P. A. Futreal, *Nature*, 2002, **417**, 949-954.
53 B. Stecca, C. Mas, V. Clement, M. Zbinden, R. Correa, V. Piguet, F. Beermann and I. A. A. Ruiz, *Proc. Nat. Acad. Sci. USA*, 2007, **104**, 5895-5900.
54 A. N. Yoshimoto, Bernardazzi, Claudio, Carneiro, Antonio Jose V., Elia, Celeste C. S., Martinusso, Cesonia A. and G. M. Ventura, Castelo-Branco, Morgana T. L., de Souza, Heitor S. P., *PLoS One*, 2012, **7**, e45332.
55 G. Chatel, C. Ganeff, N. Boussif, L. Delacroix, A. Briquet, G. Nolens and R. Winkler, *Int. J. Can.*, 2007, **121**, 2622-2627.
56 G. Bosco-Clement, F. Zhang, Z. Chen, H. M. Zhou, H. Li, I. Mikami, T. Hirata, A. Yagui-Beltran, N. Lui, H. T. Do, T. Cheng, H. H. Tseng, H. Choi, L. T. Fang, I. J. Kim, D. Yue, C. Wang, Q. Zheng, N. Fujii, M. Mann, D. M. Jablons and B. He, *Oncogene*, 2014, **33**, 2087-2097.
57 Y. Shi, X. Fu, Y. Hua, Y. Han, Y. Lu and J. Wang, *PLoS One*, 2012, **7**, e33358.
58 N. Bansal, Farley, Nadine Johnson, Wu, Lisa, Lewis, Jonathan, Youssoufian, Hagop, Bertino, Joseph R., *Mol. Can. Therap.*, 2015, **14**, 23-30.
59 T. Sheng, C. Li, X. Zhang, S. Chi, N. He, K. Chen, F. McCormick, Z. Gatalica and J. Xie, *Mol. Can.*, 2004, **3**, 29.
60 L. Mao, Y.-P. Xia, Y.-N. Zhou, R.-L. Dai, X. Yang, S.-J. Duan, X. Qiao, Y.-W. Mei, B. Hu and H. Cui, *Cancer Sci.*, 2009, **100**, 1848-1855.
61 B. N. Singh, J. Fu, R. K. Srivastava and S. Shankar, *PLoS One*, 2011, **6**, e27306.
62 J. Taipale, J. K. Chen, M. K. Cooper, B. Wang, R. K. Mann, L. Milenkovic, M. P. Scotts and P. A. Beachy, *Nature*, 2000, **406**, 1005-1009.
63 P. Chomczynski and N. Sacchi, *Nat. Prot.*, 2006, **1**, 581-585.
64 M. Frank-Kamenetsky, X. M Zhang, S. Bottega, O. Guicherit, H. Wichterle, H. Dudek, D. Bumcrot, F. Y. Wang, S. Jones, J. Shulok, L. L. Rubin and A. Porter Jeffery, *J, Biol.*, 2002, **1**, 10.
65 Y. Tang, S. Gholamin, S. Schubert, M. I. Willardson, A. Lee, P. Bandopadhayay, G. Bergthold, S. Masoud, B. Nguyen, N. Vue, B. Balansay, F. Yu, S. Oh, P. Woo, S. Chen, A. Ponnuswami, M. Monje, S. X. Atwood, R. J. Whitson, S. Mitra, S. H. Cheshier, J. Qi, R. Beroukhim, J. Y. Tang, R. Wechsler-Reya, A. E. Oro, B. A. Link, J. E. Bradner and Y.-J. Cho, *Nature Med.*, 2014, **20**, 732-740.
66 P. G. Rack, J. Ni, A. Y. Payumo, V. Nguyen, J. A. Crapster, V. Hovestadt, M. Kool, D. T. W. Jones, J. K. Mich, A. J. Firestone, S. M. Pfister, Y.-J. Cho and J. K. Chen, *Proc. Nat. Acad. Sci., USA*, 2014, **111**, 11061-11066.